Extrasolar Planets: Detection methods and Observational campaigns

Eetu Halsio
University of Oulu

Bachelor's Thesis

July 22, 2020

Contents

1 Introduction

The universe contains hundreds of billions of galaxies and each of these galaxies have hundreds of billions of stars. Many of these stars have planets as their companions and scientists are trying to search them also in hope of finding life.[1]

Planets that are orbiting another star than the Sun, are called extrasolar planets, also known as exoplanets.[2] There is a wide diversity of different extrasolar planets.[3] They are found around different kinds of stars that vary extremely from each other e.g. by temperature, mass and size[1]. Extrasolar planets can be categorized by masses, compositions and orbital elements.[2] These planets are much harder to detect than planets in the Solar System, mainly because they are so far from the Earth[3].

The First successful find of extrasolar planets happened around 1990 by radio pulsar timing (subsection 2.1)[1]. In 1995 two astronomers, Michel Mayor and Didier Queloz found the first extrasolar planet around solar-like star using ELODIE spectrograph. In 2019, they were awarded Nobel prize in Physics for their discovery. Since the first finding the research of extrasolar planets has grown considerably.

Before different kind of space campaigns were launched, most of the extrasolar planet findings have been found using the radial velocity method. Today, the most used detection method is transit photometry. Space missions like CoRoT and Kepler utilized this method to observe extrasolar planets with great success and increased greatly the number of known extrasolar planets.[1] By November 2019 there have been 4 099 confirmed extrasolar planets according to Nasa's archieve.

In this Bachelor's Thesis, I will review extrasolar planet detection methods and mention some of the well known space and ground campaigns.

2 Detection methods for Extrasolar Planets

Extrasolar planets can be detected using direct or indirect methods. Each detection method is more or less sensitive to different class of extrasolar planets and its environment.[3]

Extrasolar planets are located far from the Solar System. The closest observed extrasolar planet resides at a distance of $\sim$ 4 light-years. Planets are very faint compared to their host stars, which are so luminous that they

overshine their little companion. For such reasons, most of the methods are indirect. Indirect methods can detect extrasolar planets by observing their host star.[3] They take advantage of the planet's influence on the host star, such as temporarily reducing the host star's luminosity or causing visible motion on it by making it "wobble".

Indirect methods include e.g. pulsar and pulsating star timing, the doppler technique, astrometry, transit and microlensing, which are introduced in this thesis.

2.1 Timing Pulsars and Pulsating Stars

The first successful extrasolar planet detection was obtained through pulsar timing. Pulsars are very rapidly rotating neutron stars, stellar remnants that are formed in supernova explosions, with very strong magnetic fields.[1] They emit stable and periodic pulses of radio waves that can be observed. Typical rotation frequency is ~ 1 rotation per second but the fastest observed pulsar rotates ~ 716 rotations per second.

Observer's distance varies systematically in time, causing pulses to travel different distances. This is because the Earth rotates around the Sun and it's own axis of rotation. This variation can be taken into account and be reduced from the data, thus making the pulse signal constant.[3] The incoming signal can vary also because of the motion of the pulsar. If there is a planet with the pulsar, both rotate around their common barycenter. This motion causes a change in the distance between the pulsar and the Earth, therefore it also affects the travel time of the signal. If the pulsar has no planet, the distance between it and the Earth does not change, thus the frequency of incoming signal remains constant.

The amplitude of the variation in the pulsars period is given by the equation

$$\delta T_* = \frac{a_* sin\ i}{c} \tag{1}$$

where c is the velocity of light, a_* the semi-major axis about the barycenter and i the angle between the orbit and the plane of the sky, $i = 0$ corresponds to the face on position.[4]

The timing method does not restrict only to pulsars but can be used for pulsating stars as well. A pulsating star is a type of variable star that vary in brightness because of the expansion and the contraction of the star. The

change in the brightness can also occur if the star is in a binary system with a orbiting planet that eclipses.

Pulsar timing is a very accurate method of finding planets. By observing typical pulsars, it should be possible to detect planets with a mass from a terrestial planet up to the mass of a Jovian planet. Lower mass objects with a mass $\sim$ the Moon and larger asteroids are possible to detect in a millisecond pulsar timing residuals.[1] The precision reduces greatly for pulsating stars, therefore the minimum observable mass of a planet is larger[3].

2.2 The Doppler Technique

The Doppler technique, also known as radial velocity method, detects the excess motion, (i.e. motion of star rotating around the system's common barycenter) of a star that is caused by an orbiting planet[5]. The method utilizes the Doppler effect where the star's observed wavelengths are either blue or red shifted because of the star's radial motion with respect to the observer[6].

Gravity governs the interaction between star and planet, thus a more massive planet causes larger response in the stellar motion around the barycenter. In addition, gravity weakens with the square of the distance. Planets closer to the star induces bigger reflex motion, also their orbital period is shorter, therefore they are more easier to detect.[5]

Star's spectrum consists of numerous features that are doppler shifted. By fitting these doppler shifts it is possible to determine star's radial velocity.[3] Velocity semi amplitude K follows the equation

$$K = \left(\frac{2\pi G}{P_{orb}}\right)^{1/3} \frac{M_p sin\ i}{(M_* + M_p)^{2/3}} \frac{1}{\sqrt{1-e^2}} \tag{2}$$

where M_p the planet's mass, M_* observed star's mass, P_{orb} orbital period, G gravitational constant, e planet's orbital eccentricity and i inclination of the orbital plane respect to the plane of sky.[3]

There are some restrictions for the method. Inclination of the system is crucial in the radial velocity method. In order to doppler effect to take place, the star must have a radial motion with respect to the observer. The shifts in wavelength are not observed if the system is observed face on, i.e. $i = 0$.[4] Also stars themselves are not all suitable because of the stellar activity. Radial velocities are affected by magnetic active regions in the star.

These regions contain features e.g. spots and faculae, that impacts on the overall flux measured from the region. These regions move in and out of the sight as the star rotates affecting the measured blue- and red-shifted light.[7]

In the figure 1 is shown the radial velocity of binary star system KIC 9164561 as a function of orbital phase. In this binary system, primary A star has a mass of $\approx 2M_{\odot}$ and the white dwarf's (WD) mass was determined to be $\approx 0.197M_{\odot}$. The spectrum of the target was then cross-correlated with the spectrum of the Vega to determine the radial velocities of 11 different time points.

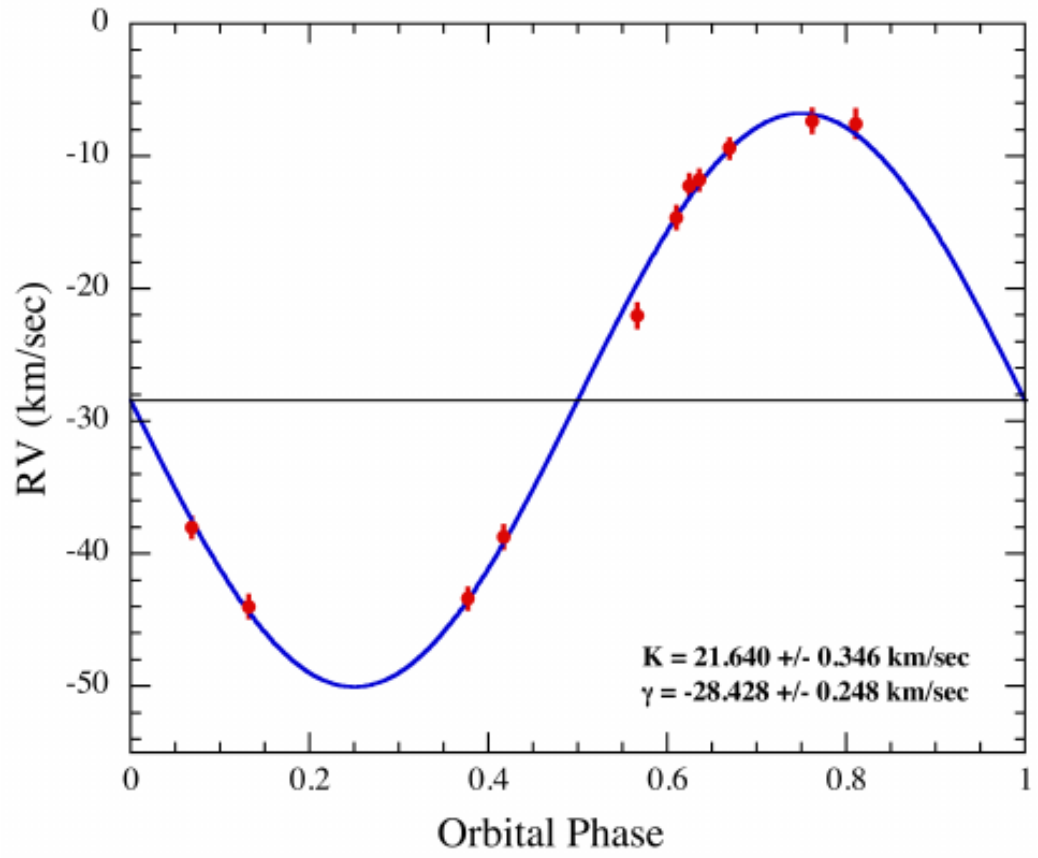

Figure 1: Radial velocity measurement for KIC 9164561 with uncertainties. Negative slope in velocity corresponds to movement towards the observer and vice versa. Sinusoidal curve represents best-fit circular orbit.[8]

2.3 Astrometry

Planets interact with stars via gravity, therefore both of the objects rotate around the system's common barycenter. The observed motion of the rotating star is projected onto the plane of the sky. This motion of the star with respect to the observer is called the wobble.

This motion is visualised in the figure 2 that shows the motion of the Sun around the common barycenter of the Solar System. The orbit with the faintest numbers illustrates the effect of Jupiter on the motion of the Sun. The green orbit with slightly more apparent numbers shows the effect of Jupiter and Saturn. The red orbit with the most apparent numbers is the sun's motion in response to the all eight planets and pluto. [3]

The motion of a planet follows Keplerian laws but instead of Keplerian orbital elements, (eccentricity e, semi-major axis a, inclination i, argument of periapsis ω and longitude of ascending node Ω), often Thiele-Innes constants (A, B, F and G) are used to linearize equations (equation (4)) for simplicity.[1]

In terms of the Keplerian elements, star's amplitude of the wobble, $\Delta\theta$, is given by equation

$$\Delta\theta \leq \frac{M_p}{M_*}\frac{a_*}{r_*} \tag{3}$$

where M_p planet's mass, M_* star's mass, a_* star's orbital semi-major axis and r_* the distance to the star from observer.[3] The wobble is more noticeable when the distance to the star is relatively short and the mass of the planet is large. Astrometry allows to solve the absolute mass of the planet and the inclination of the orbit[2].

The Thiele-Innes constants are given by equations

$$\begin{aligned}
A &= \theta(\cos\Omega\cos\omega - \sin\Omega\sin\omega\cos i)\\
B &= \theta(\sin\Omega\cos\omega + \cos\Omega\sin\omega\cos i)\\
F &= \theta(-\cos\Omega\sin\omega - \sin\Omega\cos\omega\cos i)\\
G &= \theta(-\sin\Omega\sin\omega + \cos\Omega\cos\omega\cos i)\\
C &= \theta\sin\omega\sin i\\
H &= \theta\cos\omega\sin i
\end{aligned} \tag{4}$$

where θ is signal of semi amplitude. Thiele-Innes constants together with elliptical rectangular coordinate system gives the offset of the star in an equatorial system. Elliptical coordinates are given by equation,

$$\begin{aligned}
X &= cosE - e\\
Y &= \sqrt{1-e^2}sinE
\end{aligned} \tag{5}$$

where E is the eccentricity anomaly. The offset of the star in an equatorial system is given by equations

$$\begin{aligned} x &= \Delta\delta = AX + FY \\ y &= \Delta\alpha cos\delta = BX + GY \end{aligned} \tag{6}$$

where $\Delta\delta$ is the offset in declination and $\Delta\alpha$ offset in right ascension. [9]

Equatorial coordinate system is widely used in astronomy because coordinates does not depend on the position of the observer and the time of the observation. This means, that all of the other observers can use the same set of coordinates even if their location or the time of the observation is different.

An equatorial system is used to locate objects on the celestial sphere (abstract sphere around the Earth). Object's location on the celestial sphere is given by two coordinates, declination (Dec) and right ascension (RA). Declination measures the angle (declination is measured in degrees, arcminutes and arcseconds) from celestial equator. Right ascension is measured east from the vernal equinox in the celestial equator (RA is given in hours, minutes and seconds). [10]

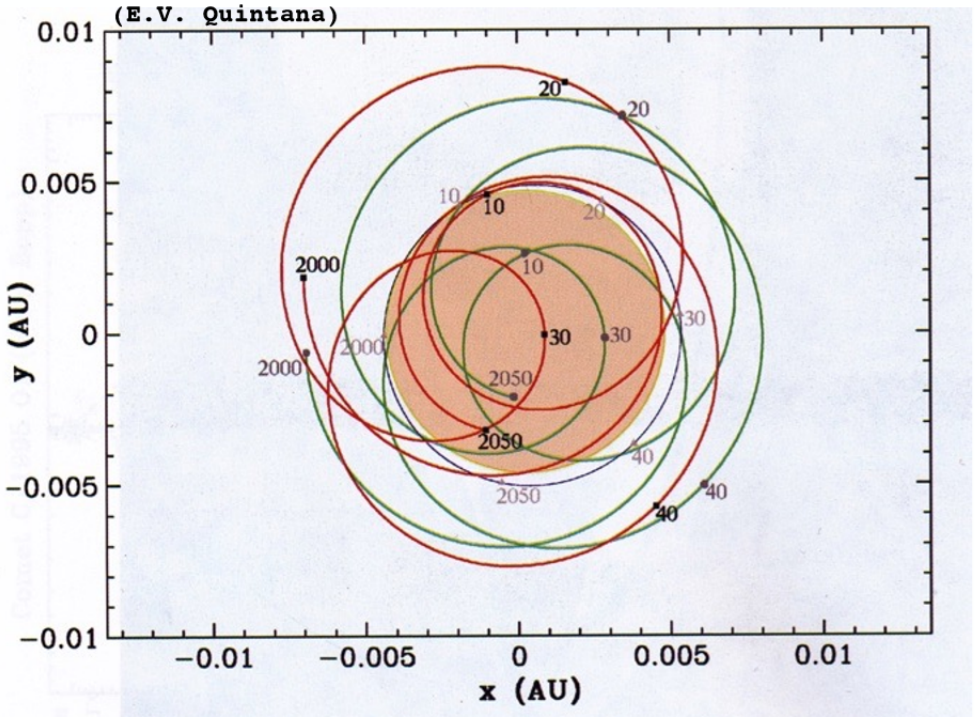

Figure 2: Motion of the Sun around the common barycenter of the Solar System. (E. V. Quintana)

Astrometry is the most sensitive method for large mass extrasolar planets and also for stars that are located within a few parsecs of the Earth.[11]

2.4 Transit Photometry

The phenomenon where a celestial object passes between another object and the observer is called transit. When a transit occurs in a front of a star, the celestial object conceals the part of the stellar disk for a limited time reducing overall flux of the star. Transit photometry utilizes this phenomenon to find planets around stars, also for a different studies, e.g. to study atmospheres.

Transit can only occur when the system is seen close to edge-on.[4] The limit of planet's orbital inclination is given by equation

$$\cos i < \frac{R_* + R_p}{r} \tag{7}$$

where R_* and R_p correspond to the star's and planet's radii, respectively, r is the distance between two objects when the planet is nearest to observer and i the angle between the orbit's normal and the line of sight.[3]

In transit, the planet reduces the flux of the observable star[9]. Transit depth is given by equation

$$\frac{\Delta F}{F} = \left(\frac{R_P}{R_*}\right)^2 \tag{8}$$

where ΔF corresponds to change in flux, F is the star's flux out of transit. Equation (7) does not take into account brightness variations in the star, e.g. limb darkening. As seen in equation (7), the transit allows the determination of the planet's radius.[12]

The probability of the transit to happen is given by equation

$$p_T = \frac{R_*}{P^{2/3}} \left(\frac{4\pi^2}{GM_*}\right)^{1/3} \tag{9}$$

where P is the planet's orbital period. Because the period depends on the planet's distance from the star, the further the planet is from the star the smaller is the probability of the transit to occur.[4]

The central transit duration i.e. equatorial crossing time is given by

$$T \equiv \frac{R_* P}{\pi a} \tag{10}$$

where a is the planet's semi-major axis.[9].

The transit method works well together with the radial velocity method introduced in the subsection 2.1. In order for a transit to occur and be observed (equation 7), the orbital inclination must be very close to edge on. In radial velocity the mass of the planet depends on $sin\ i$, thus with the transit it is possible to derive the true mass of the planet.[4] In addition, if mass and the radius of the planet is known, it is possible to determine the density of the planet[3].

2.5 Gravitational Microlensing

Einstein introduced his general theory of relativity in 1915. According to his theory, the mass distorts the space-time around it which is then felt as a gravity. This distortion then bends the incoming light from the source, i.e.

changes the direction of the light in space-time because the light follows the curvature of space-time.

Forementioned phenomenon can lead to gravitational lensing. The foreground object (the lens) bends the light that is coming from the background object (source). Gravitational lensing is recognized in two regimes, strong and weak lensing. Effects that are visible at object level are considered as strong lensing. Strong lensing has two sub-categories, macro- and microlensing. In macrolensing the lens is generally a galaxy and the source is observed as multiple resolved images or as arcs (arcs are sheared and magnified). In microlensing the angular separation of the images are too small to resolve, therefore only brightness variations of the source are observed. Weak lensing is analyzed only in statistical sense since the distortions are weak.[1]

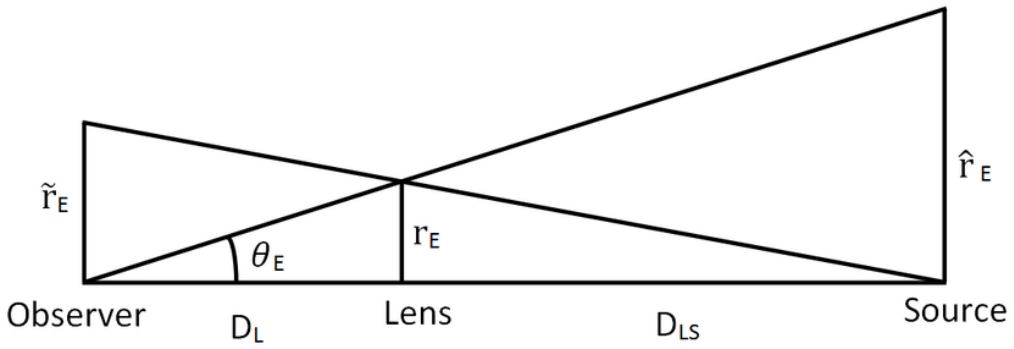

Figure 3: The geometry of gravitational lensing where the Einstein's ring r_E is projected onto the observer's plane $\tilde{r}_E$ and source's plane $\hat{r}_E$[13].

In the figure 3, one can see the gravitational lensing where the observer, lens and the source are perfectly aligned. In this special case, the images from the lensing will merge and create an Einstein ring. The radius of the ring (Einstein radius) is given by

$$r_E = \sqrt{\frac{4GM_L D_L}{c^2}} \left(1 - \frac{D_L}{D_L + D_{LS}}\right)^{1/2} \tag{11}$$

where D_L and D_{LS} are the distances from the Earth to the lens and to the source, G gravitational constant, c speed of light and M_L the mass of the lens.[3]

Microlensing is a time varying phenomenon where a projected separation between the background source and the lens (star) first decreases and then increases. In a single lens case (one foreground object) observed source will create a symmetrical lightcurve over the time, which amplitude (magnification) is determined by the angular separation of the source and the lens.[11]

Exoplanet and host star create a multiple lens case (more than one foreground object). The source's lightcurve amplitude is then asymmetrical, as can be seen in the figure 4. Exoplanets perturbs the light by their own gravitational field and create an additional deviation that appears as blimp in the lightcurve. [4]

Microlensing is a good method to observe low-mass planets, because the sensitivity extends down to 0.1 of Earth mass. The method is also most sensitive to planets at the distance of $1.4-4$ AU from their parent star. Planets closer than the minimum distance have to be found by another methods (transit and radial velocity). It is even possible to find planets around unseen stars, because the microlensing does not depend on the light from the host star. [11]

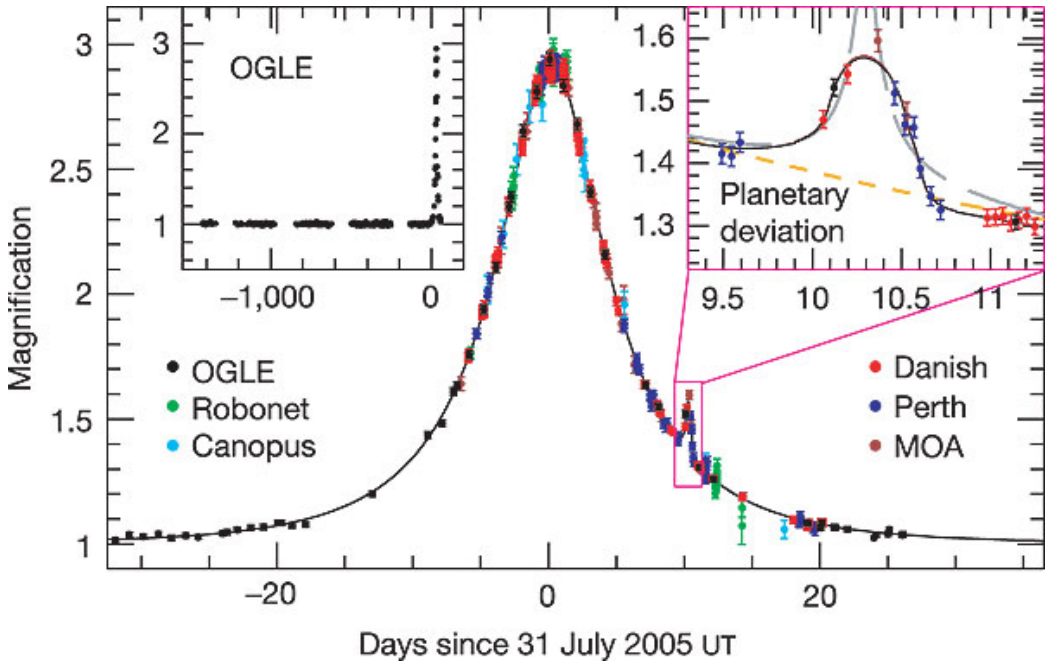

Figure 4: Observed light curve of the OGLE-2005-BLG-390 event where planetary presence shows as a peak in the light curve. Event had a red clump (cluster of red giants) as a source on whose light acted M-dwarf star (the lens star) and planetary companion.[14]

2.6 Direct Imaging

With the direct imaging method scientists try to detect incoming photons from the planet. Extrasolar planets are very faint and they reside close to their host star, which makes imaging of the planet extremely difficult due to the emission of the extremely brighter star.[9] In addition to difficulties due to the planets location, also diffraction of light by telescope optics and perturbations by Earth's atmosphere, cause their own difficulties for the imaging[3].

There are various methods to make imaging more successful. Resolving the light from different sources is easier at wider angular separation. Adaptive optics, speckle imaging and lucky imaging enhances the resolution of ground-based telescopes that are affected by Earth's atmosphere. Stellar coronagraphs (masks) are used to reduce star's flux by concealing the star.

Speckle and lucky imaging are related to each other with small differences. Both techniques uses image stacking, i.e. averages of multiple short exposures

to get a final image, while speckle averages over all of the images, whereas lucky imaging uses the best and sharpest images.[1] Figure 5 shows a fully reduced image of the planet system HR 8799.

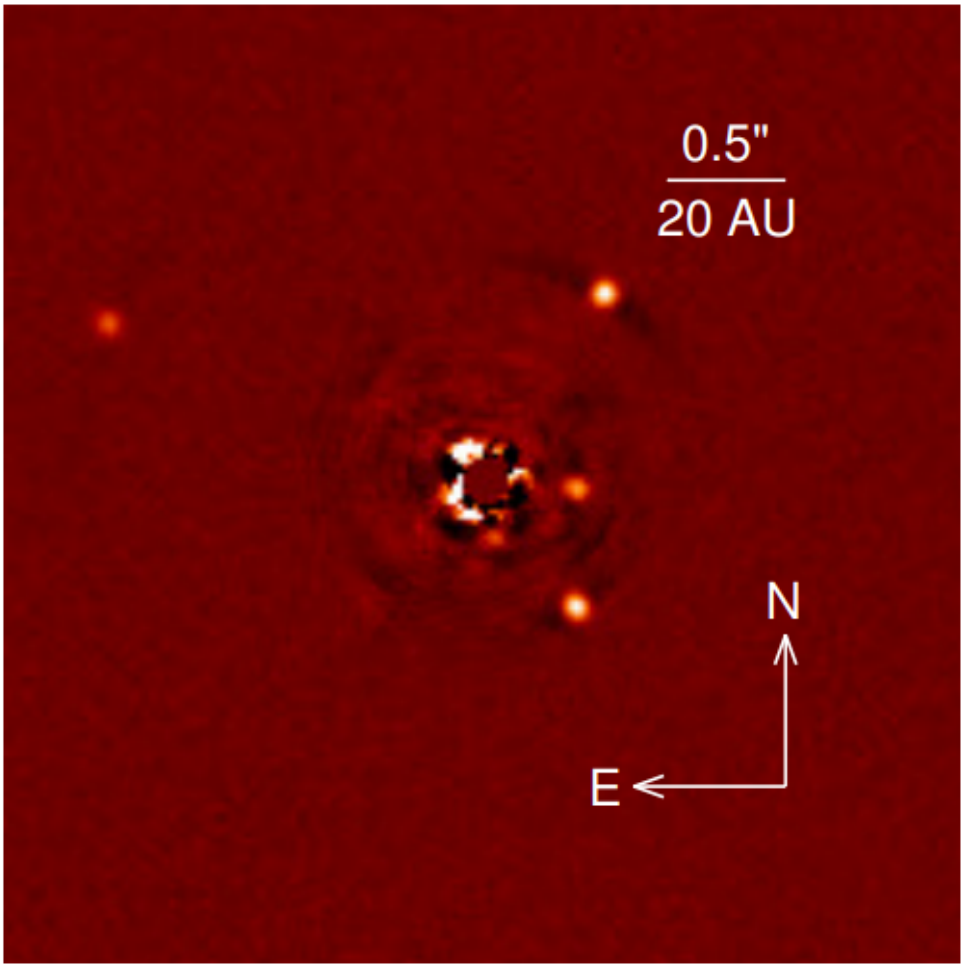

Figure 5: HR 8799 planet system. Image is taken with LMIRCam in L' band[15].

3 Campaigns

Since the first results of exoplanet discoveries in 1990, the science of extra-solar planets started to get recognition and to become a very respectable

field in the science community. First discoveries were found by ground-based observations using the radial velocity method.[1] The number of extrasolar planets remained low until space-based observations began to search extrasolar planets in large-scale by utilizing planetary transit.[16]

3.1 Past and ongoing space based campaigns

3.1.1 CoRoT

The CoRoT, Convection, Rotation and planetary Transits, was launched on 2006 December 27th on a polar orbit of the Earth. Mission lasted 7 years from 2006 to 2013. Mission was led by French Space Agency (CNES) together with European Space Agency (ESA) and other European countries. CoRoT mission had two major scientific programmes, stellar seismology and the search of extrasolar planets, making it the first space telescope that was dedicated to the search of the extrasolar planets. CoRoT detected extrasolar planets by the transit method (subsection 2.4) where the observed stellar flux decreases when the planet crosses between the star and the observer.

The CoRot telescope has a 2.7° x 3.05° field of view. The focal plane consists of 4 CCDs (seen in the figure 6). CCDs are inside a focal box that protects against radiation by a 10mm aluminium shield. Focal box has a window in front that lets the light from the targets through.[17]

CoRoT performed observations of extrasolar planets and stellar seismology simultaneously by dividing CCDs between the programmes. CCDs are thinned back illuminated (collects charge through thinned backside of CCD and performs better in the blue and UV wavelength region[18]) and they consists of 2048x2048 pixels with a size of $15\mu m$. Each of the detectors could observe up to 6000 targets simultaneously [19]. Number of confirmed exoplanets found by CoRoT is currently 37 [20].

Further information available at mission website: `https://corot.cnes.fr/fr/` and at database website `http://idoc-corot.ias.u-psud.fr/sitools/client-user/COROT_N2_PUBLIC_DATA/project-index.html`.

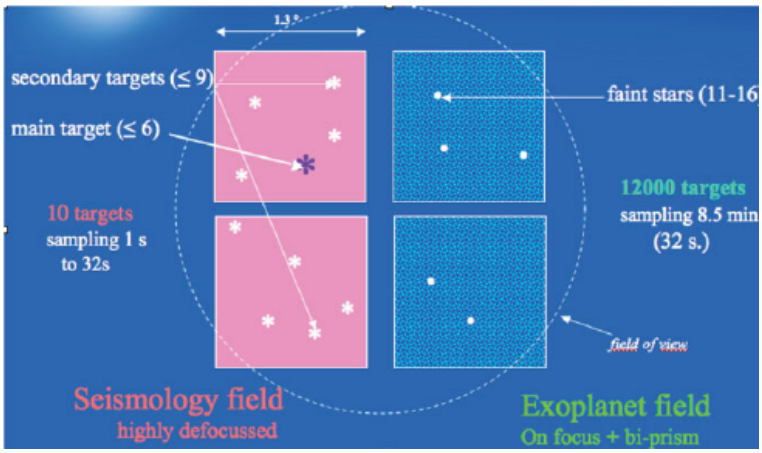

Figure 6: The focal plane of CoRoT and it's 4 CCDs. The number of targets in the given field are given together with a sampling time. Numbers are colored after CCDs that correspond to either seismology or exoplanet field.[19]

3.1.2 Kepler

The Kepler space telescope was launched back in 2009 by United States National Aeronautics and Space Administration (NASA) and the mission lasted until 2013. Kepler was the first telescope that was meant for large-scale extrasolar planet detection. The Kepler mission was designed to find Earth-like extrasolar planets in the habitable zone around a wide variety of stars. Planets that reside in the habitable zone are more likely to harbour life because the temperature allows the water to be in liquid form.[21] Kepler used transit photometry (subsection 2.4) as a detection method, as this method determines the planet's orbital period and size. Combining transit photometry with radial velocity method (subsection 2.2) allows determination of the planet's mass and density. Combination of these methods provides valuable information about the planet and makes the transit an excellent choice in space-based observation.[22]

The Kepler spacecraft was equipped with a 0.95m Schmidt telescope, 110 $\deg^2$ field of view and 4 reaction wheels that kept the poining of the telescope extremely presice. Due to its large field of view Kepler managed to target simultaneously $\sim$ 150,000 star systems, thus increasing the likelihood of observing a transit.[23]

The requirement for a true planet detection was at least three transits with steady parameters, such as period and brightness. Therefore, the requirement for the mission length was given to be at least three years.[21]

In the Figure 7, I have plotted the orbits of planets from the vetted Exoplanet Orbit Database[24]. Correlation can be seen between the eccentricity dispersion and orbital period. This would be likely, because of the larger tidal circularization timescales on high period orbits.[25] Total number of confirmed planets found by Kepler is 2347[24].

Further information available at mission website: `https://www.nasa.gov/mission_pages/kepler/main/index.html` and at database website `https://exoplanetarchive.ipac.caltech.edu/docs/counts_detail.html`

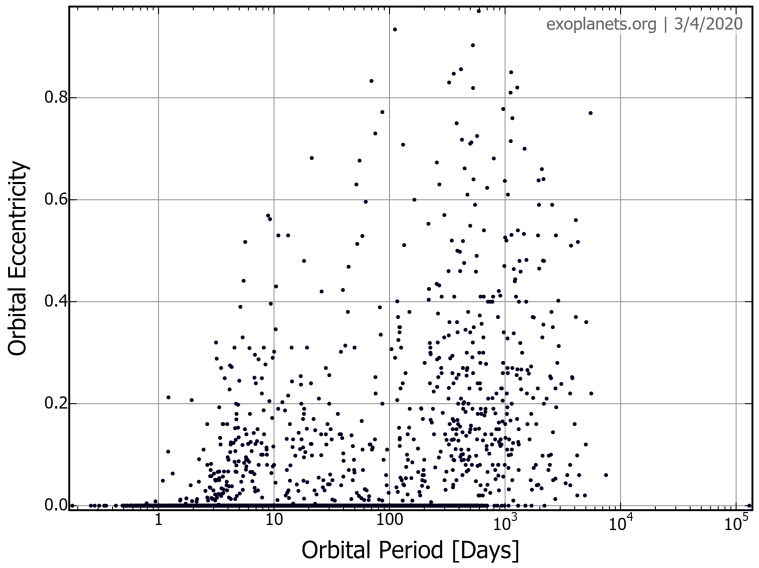

Figure 7: Orbital eccentricity of exoplanets vs orbital period, including Kepler Candidates (confirmed and unconfirmed)[26].

3.1.3 K2

The Kepler mission was continued as the K2 mission from 2013 until 2018. This is because Kepler lost two of it's reaction wheels. As a consequence Kepler could not keep it's orientation as accurate as during the Kepler mission for extended periods of time but alternative ways to compensate the loss of

reaction wheels was developed.[23] In the K2 mission, Kepler used Solar radiation pressure for stabilization by pointing near ecliptic and by using thrusters to reduce drift. This stabilization enabled Kepler to observe one field for $\sim$ 75 days before the telescope had to be turned away from the sun.[27] The total number of confirmed planets discovered by K2 is 397[24].

Further information available at mission website: `https://www.nasa.gov/mission_pages/kepler/main/index.html` and at database website `https://exoplanetarchive.ipac.caltech.edu/docs/counts_detail.html`

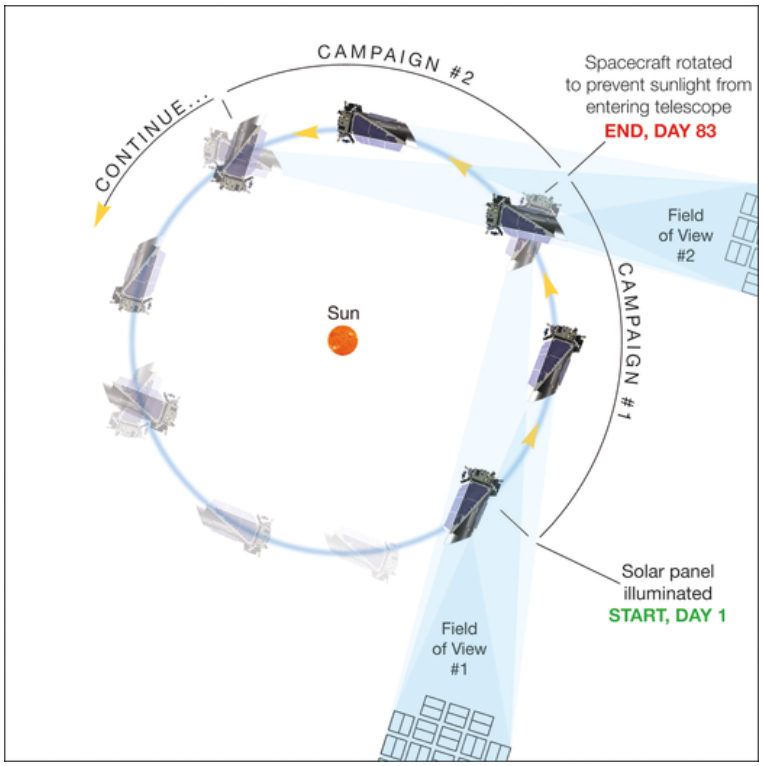

Figure 8: Individual campaigns of the K2 mission.[23].

3.1.4 TESS

TESS, The Transiting Exoplanet Survey Satellite launched on 2018 April 18th[28]. It is NASAS's new space telescope in the search of extrasolar planets and the successor of the Kepler telescope. TESS's detection method

is transit photometry (subsection 2.4), which was proven to be an extremely efficient method to find planets that were not detected by Kepler. Unlike Kepler, TESS performs observations of five nearby stars with the primary object of finding transiting planets that are smaller than Neptune. On top of finding planets, it observes stars bright enough to possibly follow-up with the spectroscopic observation to analyze the atmospheric composition of the planet and to measure the planetary mass.[29]

TESS has a 13.7 day period high earth elliptical orbit. It is equipped with four $24^\circ \times 24^\circ$ field of view cameras that together have a sky coverage of $96^\circ \times 24^\circ$ (a sector that is composed of four aligned cameras as seen in the Figure 8.) for 27.4 days per pointing. Primary mission time is 2 years and in the first half of it TESS will perform observations of 13 sectors in the southern ecliptic hemisphere and the second year in the northern ecliptic hemisphere.[28] Total confirmed planets found by TESS is 41[24].

Further information available at mission website: `https://tess.mit.edu/` and at database website `https://exoplanetarchive.ipac.caltech.edu/docs/counts_detail.html`

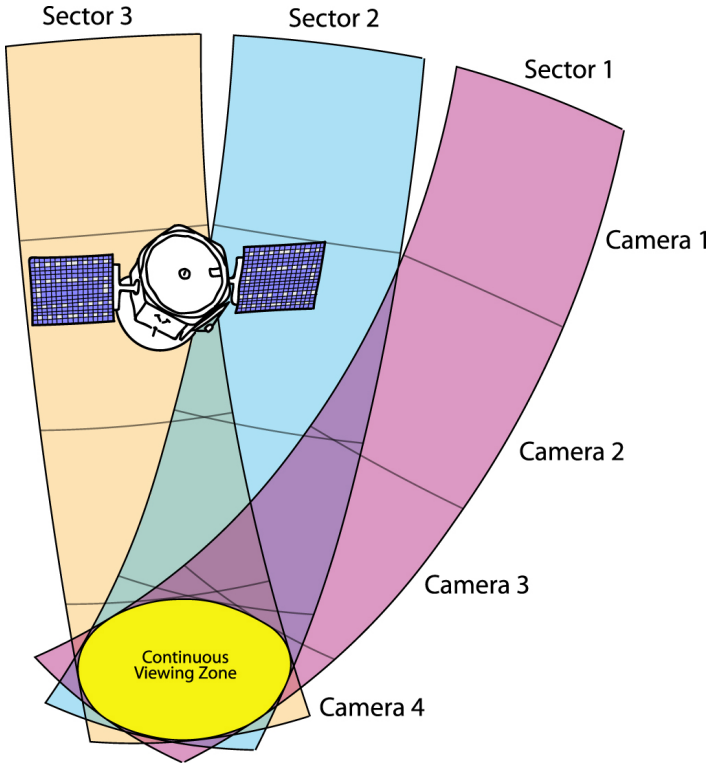

Figure 9: TESS's observation illustrated with three sectors, where the fourth camera is centered continuously on the ecliptic pole. TESS rotates $\sim 28°$ around the longitudal axis that is aligned with a fixed ecliptic longitude. Rotation happens after two orbital periods.[28]

3.1.5 GAIA

Gaia spacecraft is ESA's ambitious mission to survey a large part of the stars of the Milky Way galaxy. It was launched on 2013 December 19th and it was positioned on the second Lagrangian point of Sun-Earth-Moon system. It remained in this gravitationally unstable point for it's mission length that was 5 years.[30] However, due to fuel reserve onboard, GAIA is expected to operate until 2024[31].

Gaia has many scientific goals that are related to get better understanding about stellar/galaxy evolutions and physics, but it also utilizes its great astrometric capabilities to observe planetary systems. Through these observations, it is possible to obtain parameters that are not possible to get by

other means. Astrometry (subsection 2.3) is quite limited to observation of at least Jupiter-mass planets in planetary systems, but this makes it possible for future observations to search terrestial planets in the habitable zone that are protected by a giant planet in a more distant orbit. This method with Gaia also provides the actual masses of planets rather than a lower limit, like in the case of the radial velocity.[30]

Mission website: `https://sci.esa.int/web/gaia/`

3.1.6 CHEOPS

CHEOPS, CHaracterizing ExoPlanet Satellite, was launched on 2019 December 19th. CHEOPS was completed with a partnership between ESA and Switzerland. In addition, it had multiple major contributions from other European countries. CHEOPS was chosen as a first Small-class mission (S1) in ESA's Science programme.[32] Mission is planned for a duration of 3.5 years and it is estimated that $\sim$ 500 targets will be observed. The main scientific objective is to study the structure of extrasolar planets, that are smaller in size than Saturn and are orbiting around known bright stars.

CHEOPS will use transit photometry (subsection 2.4) to determine accurate radii of the planet whose mass is already estimated through ground-based observations with the radial velocity method (subsection 2.2). CHEOPS will identify planets that have a strong atmospheres. It can constrain the critical core mass (pinpoint those planets that have experienced runaway gas accretion) as a function of the distance to the host star, metallicity and mass, especially for planets that do not reside very close to the host star. The CHEOPS will orbit in a Sun Synchronous Low Earth Orbit (LEO) and will perform observations by targeting individual objects. Typical pointing time is $\sim$ 6 to 12 hours.[33]

Mission website: `https://cheops.unibe.ch/`

3.2 Past and ongoing ground based campaigns

3.2.1 WASP

WASP, Wide Angle Search for Planets, consortium was established back in 2000 by group of astronomers (mostly from UK) and it is still active. There are two SuperWASP systems in the world and they are located at Roque de los Muchachos Observatory on the Canary islands and at the South African

Astronomical Observatory in Sutherland. Multi-detector SuperWASP cameras are wide-field imaging systems.

SuperWASP systems have an equatorial mount and they can have multiple cameras from 1 to 8. Each system has a 482 $\deg^2$ field of view. The whole system is capable of monitoring the sky every 40 minutes.

SuperWASP systems uses transit photometry (subsection 2.4) as a detection method to observe simultaneously thousands of stars down to visual magnitude of $\sim$ 15. Main goal of the observations are to search suitable transiting planetary systems for spectroscopic observations.[34]

Further information available at mission website: `https://wasp-planets.net/`

3.2.2 OGLE

OGLE, the Optical Gravitational Lensing Experiment, project began in 1992 and it is still going on.[35] OGLE is located at the Las Campanas Observatory, Chile[13]. It belongs to the first generation of microlensing sky surveys and it focuses on sky variability. OGLE's main objective is to observe gravitational microlensing events (subsection 2.5). Extrasolar planets can be found this way because of their interaction with light that is passing through the planetary system. This interaction can be seen in the figure 4.

OGLE is now in it's fourth phase. The instruments have been upgraded every time OGLE has moved into another observation phase. OGLE-IV uses a 1.3-m Warsaw telescope that is designed as Ritcher-Crétien with three lens field corrector. The telescope has a large $\sim 1.5^\circ$ fov and OGLE-III camera utilized only $\sim 25\%$ of this. It was only natural to maximise the usage of the fov to observe sky even more efficiently. This led into a design in form of a mosaic with 2048×4102 pixel CCDs with a pixel size of $15\mu m$. [35]

Further information available at mission website: `http://ogle.astrouw.edu.pl/main/main.html`

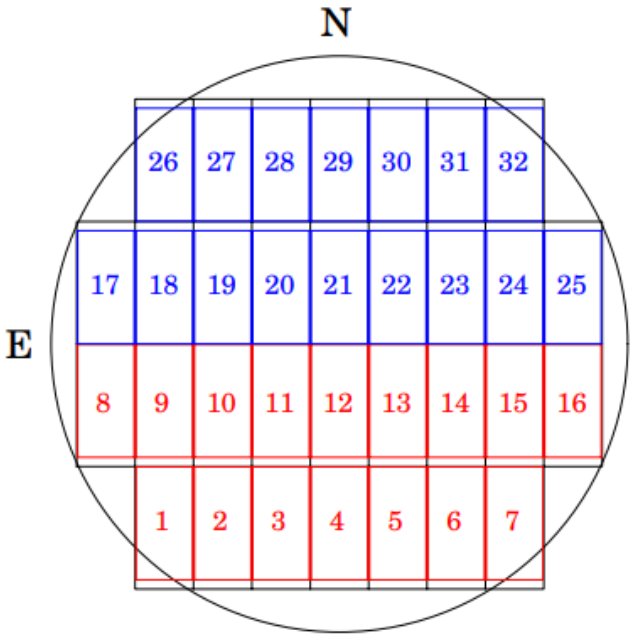

Figure 10: OGLE-IV field of view that is filled by 32 detectors. N and E indicate sky directions. [35].

3.2.3 HARPS

The HARPS, High Accuracy Radial Velocity Planet Searcher, project began in 1998 by ESO. In 2003 ESO received HARPS, that is an echelle spectrograph which was installed on ESO's 3.6 m Telescope at La Silla Observatory in Chile.

HARPS produces high-resolution wavelength calibrated spectra (spectra which lines are identified to correspond certain wavelength) together with radial velocity of the stellar object. HARPS contains two fibres, one for the object and one for the reference. These fibres transfer the light for the spectrograph together with a calibration lamp. Spectrograph's optics re-image the feed from the fibers onto mosaic that is constructed of two 4096×4069 pixel CCDs. The wavelength interval that the spectra cover is 380nm to 690nm.[36]

Mission information can be found at `https://www.eso.org/sci/facilities/lasilla/instruments/harps.html`

3.3 Upcoming space based campaigns

3.3.1 JWST

JWST, The James Webb Space Telescope, will be launched in 2021 and the mission is expected to revolutionize our knowledge of extrasolar planets with transit photometry (subsection 2.4).[37] JWST is being developed by NASA together with major contributions from ESA and Canadian Space Agencies (CSA)[38]. It will be the most powerful space telescope and it will include spectroscopes to examine molecular composition and structure of atmospheres.[37] JWST will do this for a wide diversity of planets from gas giants to super-Earths. JWST's main science goals are divided into four themes: First light and reionization, assembly of galaxies, birth of stars and protoplanetary systems and planetary systems and origins of life.

In the first light and reionization, also known as The End of the Dark Ages, one of the primary goals of observations is to find the first luminous sources that formed in the beginning of time and to determine the ionization history of the universe.

The Assembly of Galaxies will focus on the study of galaxies and their formation through time till the present time.

In The Birth of Stars and Protoplanetary Systems, main objective of JWST is to study stars, especially how they are born and why most of the stars are born in star groups.

Formation of Planetary Systems and the Origin of Life theme will focus on the planetary systems. JWST's main goal is to study chemical compositions of such systems and to determine their potential for origins of life. [39]

JWST will be stationed to halo orbit in the second Earth-Sun Lagrangian point. This orbit provides stable and uninterrupted observation for the telescope.[37] JWST mission time is planned to last 5 years but it can be extended to 10 year mission due to extra fuel reserve. During the first year of mission, JWST may be able to characterize over 50 atmospheres of exoplanets. Extrapolating over the full mission time, this would indicate that JWST could characterize over 475 planets.[40]

Observations will be performed with it's 4 instruments, a near IR-camera, a near IR-multiobject spectrograph and a filter imager that covers a wavelength span of 0.6 - 5.0 μm. A sunshield will keep these instruments safe by providing thermal control.[41]

Further information available at mission websites:

https://www.jwst.nasa.gov/
https://sci.esa.int/web/jwst/
https://www.asc-csa.gc.ca/eng/satellites/jwst/
http://www.stsci.edu/jwst/

4 Conclusions

The future of extrasolar planet search is bright. Many planets have been found already and extremely efficient telescopes are launching in the coming years. Detection methods are primarily the same. Transit method has already been proven to be extremely powerful and it will be used as the leading method in the coming missions. We do not currently have much knowledge according to extrasolar planets but these new telescopes will find and observe planets better than ever. This new information will help us to understand the formation and evolution of planets. Addition to planet formation, every new piece of information about planets will help us to understand origin of life and possibly to find life itself outside of planet Earth. Coming years in the field of extrasolar planets will be extremely interesting and possibly full of surprises.

References

[1] Perryman M. The exoplanet handbook. 2nd ed. University Printing House, Cambridge CB2 8BS, United Kingdom; 2018.

[2] Irwin PGJ. Exoplanets: Detection, Formation, Properties, Habitability. Mason JW, editor. Springer, Berlin, Heidelberg; 2008.

[3] de Pater I, Lissauer JJ. Planetary Sciences. Updated second ed. University Printing House, Cambridge CB2 8BS, United Kingdom; 2015.

[4] Ollivier M, Encrenaz T, Roques F, Selsis F, Casoli F. Planetary systems: Detection, Formation and Habitability of Extrasolar Planets. Börner G, Burkert A, Burton WB, Dopita MA, Eckart A, Encrenaz T, et al., editors. Springer-Verlag Berlin Heidelberg; 2009.

[5] Fischer DA, Howard AW, Laughlin GP, Macintosh B, Mahadevan S, et al. Exoplanet Detection Techniques. ArXiv:150506869v2. 2015.

[6] Wright JT. Radial Velocities as an Exoplanet Discovery Method. arXiv:170707983. 2017.

[7] Nava C, López-Morales M, Haywood RD, Giles HAC. Exoplanet Imitators: A test of stellar activity behavior in radial velocity signals; 2019.

[8] Rappaport S, Nelson L, Levine A, Sanchis-Ojeda R, Gandolfi D, Nowak G, et al. Discovery of Two New Thermally Bloated Low-Mass White Dwarfs Among the Kepler Binaries. The Astrophysical Journal. 2015 02;803.

[9] Wright JT, Gaudi BS. Exoplanet Detection Methods. ArXiv:12102471v2. 2012.

[10] Cosmos, The SAO encyclopedia;. Available from: `https://astronomy.swin.edu.au/cosmos/E/Equatorial+Coordinate+System`.

[11] Mason JW, editor. EXOPLANETS: Detection, Formation, Properties, Habitability. Springer, Praxis Publishing Ltd, Chichester, UK; 2008.

[12] Moutou C, Pont F. Detection and characterization of extrasolar planets: the transit method. Ecole de Goutelas. 2005.

[13] Freeman M, Philpott L, Abe F, D Albrow M, P Bennett D, Bond I, et al. Can the Masses of Isolated Planetary-mass Gravitational Lenses be Measured by Terrestrial Parallax? The Astrophysical Journal. 2015 01;799:181.

[14] Beaulieu JP, P Bennett D, Fouqué P, Williams A, Dominik M, Jorgensen U, et al. Discovery of a Cool Planet of 5.5 Earth Masses Through Gravitational Microlensing. Nature. 2006 02;439:437–40.

[15] Maire, A -L , Skemer, A J , Hinz, P M , Desidera, S , Esposito, S , Gratton, R , et al. The LEECH Exoplanet Imaging Survey. Further constraints on the planet architecture of the HR 8799 system. A&A. 2015;576:A133.

[16] Basri G, Borucki WJ, Koch D. The Kepler Mission: A wide-field transit search for terrestrial planets. New Astronomy Reviews. 2005;49(7):478 – 485. Wide-Field Imaging from Space.

[17] Auvergne M, Bodin P, Boisnard L, Buey JT, Chaintreuil S, Epstein G, et al. The CoRoT satellite in flight: description and performance. Astronomy & Astrophysics. 2009;506(1):411–424.

[18] Lesser M. A Summary of Charge-Coupled Devices for Astronomy. Publications of the Astronomical Society of the Pacific. 2015 nov;127(957):1097–1104. Available from: https://doi.org/10.1086%2F684054.

[19] Baglin A, Auvergne M, Barge P, Deleuil M, et al. CoRoT: Description of the Mission and Early Results. Proceedings of the International Astronomical Union. 2008 05;4:71 – 81.

[20] IAS CoRoT Public Archieve;. Available from: http://idoc-corot.ias.u-psud.fr/sitools/client-user/COROT_N2_PUBLIC_DATA/project-index.html.

[21] Koch DG, Borucki WJ, Basri G, Batalha NM, Brown TM, Caldwell D, et al. Kepler Mission Design, Realized Photometric Performance, and Early Science. The Astrophysical Journal Letters. 2010;713:L79.

[22] Jenkins JM, Caldwell DA, Chandrasekaran H, Twicken JD, Bryson ST, Quintana EV, et al. OVERVIEW OF THEKEPLER-SCIENCE PROCESSING PIPELINE. The Astrophysical Journal. 2010 mar;713(2):L87–L91.

[23] Howell SB, Sobeck C, Haas M, Still M, Barclay T, Mullally F, et al. The K2 Mission: Characterization and Early Results. Publications of the Astronomical Society of the Pacific. 2014;126(938):398–408.

[24] NASA exoplanet archieve;. Available from: https://exoplanetarchive.ipac.caltech.edu/docs/counts_detail.html.

[25] Kane S, Gelino D. The Habitable Zone and Extreme Planetary Orbits. Astrobiology. 2012 10;12:940–5.

[26] Exoplanets Data Explorer;. Available from: http://exoplanets.org/plots.

[27] Vanderburg A, Johnson JA. A Technique for Extracting Highly Precise Photometry for the Two-WheeledKeplerMission. Publications of the Astronomical Society of the Pacific. 2014 oct;126(944):948–958.

[28] Barclay T, Pepper J, Quintana EV. A Revised Exoplanet Yield from the Transiting Exoplanet Survey Satellite (TESS). The Astrophysical Journal Supplement Series. 2018 oct;239(1):2.

[29] Ricker GR, Winn JN, Vanderspek R, Latham DW, Bakos G, et al. Transiting Exoplanet Survey Satellite. Journal of Astronomical Telescopes, Instruments, and Systems. 2014;1(1):1 – 10 – 10.

[30] Gaia Collaboration, Prusti, T , de Bruijne, J H J , Brown, A G A , Vallenari, A , Babusiaux, C , et al. The Gaia mission. A&A. 2016;595:A1.

[31] Pancino E. Gaia: The Galaxy in six (and more) dimensions. Advances in Space Research. 2020;65(1):1 – 10. Available from: http://www.sciencedirect.com/science/article/pii/S0273117719307987.

[32] Asquier J, Rando N, Van Damme CC, Ratti F, Isaak K, Southworth R, et al. CHEOPS: the ESA mission for exo-planets characterization ready for launch. digitalcommonsusuedu. 2019.

[33] Broeg, C , Fortier, A , Ehrenreich, D , Alibert, Y , Baumjohann, W , Benz, W , et al. CHEOPS: A transit photometry mission for ESA's small mission programme. EPJ Web of Conferences. 2013;47:03005.

[34] Pollacco DL, Skillen I, Cameron AC, Christian DJ, Hellier C, Irwin J, et al. The WASP Project and the SuperWASP Cameras. Publications of the Astronomical Society of the Pacific. 2006 oct;118(848):1407–1418.

[35] Udalski A, Szymański MK, Szymański G. OGLE-IV: Fourth Phase of the Optical Gravitational Lensing Experiment; 2015.

[36] PHASE C. Setting new standards with HARPS. The Messenger. 2003;114:20.

[37] Beichman C, Benneke B, Knutson H, Smith R, Lagage PO, Dressing C, et al. Observations of Transiting Exoplanets with the James Webb Space Telescope (JWST). Publications of the Astronomical Society of the Pacific. 2014 dec;126(946):1134–1173.

[38] Gardner JP, Mather JC, Clampin M, Doyon R, Greenhouse MA, Hammel HB, et al. The James Webb Space Telescope. Space Science Reviews. 2006 Nov;123(4):485–606. Available from: http://dx.doi.org/10.1007/s11214-006-8315-7.

[39] Lightsey PA, Atkinson CB, Clampin MC, Feinberg LD. James Webb Space Telescope: large deployable cryogenic telescope in space. Optical Engineering. 2012;51(1):1 – 20.

[40] Fortenbach CD, Dressing CD. A Framework For Optimizing Exoplanet Target Selection For The James Webb Space Telescope. Publications of the Astronomical Society of the Pacific. 2020 mar;132(1011):054501. Available from: https://doi.org/10.1088%2F1538-3873%2Fab70da.

[41] P Gardner J, Mather J, Clampin M, Doyon R, Greenhouse M, Hammel H, et al. The James Webb Space Telescope. Space Science Reviews. 2009 02;123:485–606.